Aubry transition with small distortions

O. Cépas and P. Quémerais
Institut Néel, CNRS, Université Grenoble Alpes, Grenoble 38000, France

(Received 14 April 2024; accepted 3 September 2024; published 15 October 2024)

We show that when the Aubry transition occurs in incommensurately distorted structures, the amplitude of the distortions is not necessarily large as suggested by the standard Frenkel-Kontorova mechanical model. By modifying the shape of the potential in such a way that the mechanical force is locally stronger (i.e., increasing the nonlinearities), the transition may occur at a small amplitude of the potential with small distortions. A phason gap then opens, while the phonon spectrum resembles a standard undistorted spectrum at higher energies. This may explain the existence of pinned phases with very small distortions as experimentally observed in charge-density waves.

DOI: 10.1103/PhysRevE.110.044206

I. INTRODUCTION

The Aubry transition is an equilibrium phase transition at zero temperature between two distinct incommensurately modulated phases, driven by changes in model couplings [1,2]. The two phases differ in their degeneracies. One phase, called the sliding phase, has a continuous degenerate manifold of ground states which allows their sliding at no energy cost. In the other phase, called pinned phase, the degeneracy is lifted and the ground state manifold becomes discontinuous (and is the Cantor space of Aubry-Mather [2,3]). In this case, the symmetry-related ground states are separated by energy barriers, which make them pinned in space. The Aubry transition can thus be viewed as a pinning transition. It was originally called the transition by breaking of analyticity [1,2] because the envelope function of the modulation (also called the hull function) changes from continuous in the sliding phase to discontinuous in the pinned phase when nonlinear effects in the model become large enough. Originally, the Aubry transition has been discussed in the one-dimensional mechanical Frenkel-Kontorova model [1,2] and later in various models where two length scales are in competition [4,5].

The question of its experimental relevance is still largely open. Given the generality of the model, it has been claimed to apply in different contexts: it has been invoked in the question of friction and the possibility of having superlubric sliding phases—for example, in two rotated graphene planes that may slide one over the other with low friction [6], at incommensurate boundaries of solids [7], or for a tip sliding over a surface either in a stick slip or continuous manner [8]. More recently, it has been observed and discussed in artificial systems of cold atoms subjected to a periodic optical potential [9], or in two-dimensional colloidal monolayers [10]. The first application of Aubry's theory was discussed for incommensurate charge-density waves in some solids [11,12], which are pinned in the absence of an external electric field [13]. It was argued that the observed pinning may be an intrinsic effect and the consequence of the Aubry transition [11,12]. However, the distortions measured experimentally are generally small, of the order of a few percent of the lattice spacing [14]. On the other hand, in the Aubry pinned phase (above the transition at strong enough coupling to the potential), the distortions are predicted to be large. For example, in the Frenkel-Kontorova model, they are typically of the order of tens of percent of the bond length at the transition and even larger above the transition [11,12]. The same phenomenon occurs in electronic models of charge-density waves [11,12,15]. This discrepancy in the distortions, of an order of magnitude, makes it difficult to reconcile Aubry's theory with experiments. As a consequence extrinsic sources of pinning, i.e., pinning by impurities, have been invoked to explain charge-density waves, but they may not be necessary. The theoretical issue that we study here by introducing a modified Frenkel-Kontorova model is to understand whether pinning is necessarily accompanied by large distortions, or, in other words, if it is possible to have an incommensurately distorted phase, with small distortions, yet pinned.

The question of disentangling distortions and pinning is not simple as both occur as consequences of the presence of the nonlinear potential in the standard Frenkel-Kontorova model. By introducing a second length scale, in competition with the first, the potential distorts the regular structure. At the same time, by breaking the translation symmetry that ensures the existence of the sliding phase, the potential induces pinning. It is further known that the latter occurs above a threshold of the amplitude of the nonlinear potential. On the other hand, the sliding incommensurate phase remains stable below this threshold as a consequence of the Kolmogorov-Arnold-Moser (KAM) theorem [16] which thus generally prevents a pinned phase with small distortions.

Let us consider two extreme and opposite situations. First, there are models, such as that of Brazovskii, Dzyaloshinskii, and Krichever [17], which exhibit a form of super-stability: the sliding phase is stable for all values of the nonlinear coupling. It is then impossible to have a pinned phase (*a fortiori* with small distortions). This behavior is special, as it is the consequence of the integrability of the model: once the integrability is broken, the Aubry transition occurs [15]. Second, if the conditions of the KAM theorem are not fulfilled by the nonlinear term, there is no mathematical ground to have

a sliding phase: the threshold of the Aubry transition could vanish. The first condition to apply the KAM theorem is that the perturbation of the integrable dynamical system must be small enough [18]. In the present case, this perturbation is the derivative of the potential (see Sec. II) which must thus remain everywhere small enough. If the derivative were locally diverging for example, the KAM theorem would not apply. The strategy is therefore to choose a smooth potential that would develop a singularity under deformation in some limit. Several choices are possible, depending on which derivative should be singular [18], and we will choose the simplest one with a locally large first derivative. By continuity, we expect (and we will check) that the threshold of the Aubry transition is strongly reduced for such modified potentials. As a matter of fact, there has been interest over the years in modifying either the interatomic potentials [19–21] or the external periodic potentials [22] but the present issue has not been discussed.

The paper is organized as follows: in Sec. II, we introduce the modified model that is characterized by an amplitude and a shape parameter that induces locally large derivatives. We study its Aubry transition (i.e., how the pinning is affected) and the distortions both analytically and numerically in Sec. III. In Sec. IV, we compute the phason gap that opens up at the transition and compute, more generally, how the phonon spectrum evolves.

II. MODIFICATION OF THE FRENKEL -KONTOROVA MODEL

The modified classical Frenkel-Kontorova model we consider here reads

$$W(\{x_n\}) = \frac{1}{2}\sum_n (x_{n+1} - x_n - \mu)^2 + \frac{K}{(2\pi)^2}\sum_n V_\alpha(x_n), \quad (1)$$

where x_n are the continuous physical variables and K, ,α and μ some parameters. x_n is typically the position of an atom n constrained to be along a linear chain. Here, the first term of W is a local approximation of an interatomic potential which has a minimum at μ. μ can be regarded as tunable, for example, by an external applied force. The second term is a periodic substrate (or interaction) potential with an amplitude controlled by K. Its period is chosen to be 1 (this sets the unit of length with no loss of generality),

$$V_\alpha(x+1) = V_\alpha(x). \quad (2)$$

The continuous translation invariance in the absence of the potential, $x_n \to x_n + \phi$ where ϕ is any real number, is now broken by the potential.

We consider the modified potential,

$$V_\alpha(x) = \frac{\cosh\alpha\cos(2\pi x) - 1}{\cosh\alpha - \cos(2\pi x)}, \quad (3)$$

which depends on a real parameter $\alpha > 0$ that controls the shape (see Fig. 1 and some details in Appendix A). When $\alpha \to +\infty$, $V_\alpha(x) \to \cos(2\pi x)$, giving the standard Frenkel-Kontorova model [1]. When $\alpha \to 0$, the potential is more strongly peaked at integers. This choice is interesting because its derivative becomes locally large when α is small. Its

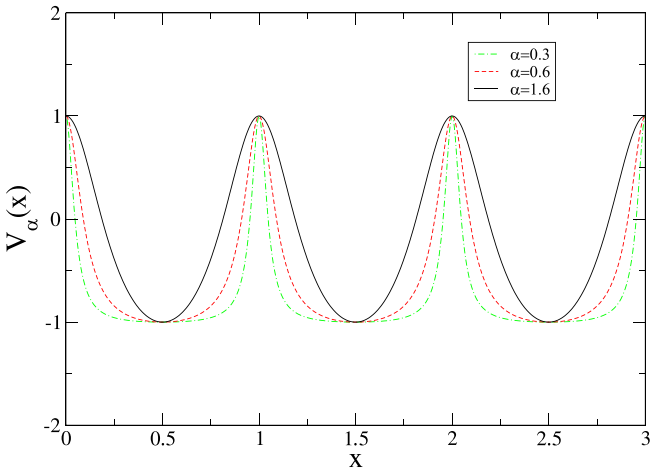

FIG. 1. Modified periodic potential $V_\alpha(x)$ for various α. When $\alpha \to +\infty$, the potential $V_\alpha(x) \to \cos(2\pi x)$, which is the standard Frenkel-Kontorova model. For small α, its derivative becomes locally large.

maximum is indeed given by (see the Appendix A)

$$V'_\alpha(x_0) = \frac{9\pi}{2\sqrt{3}}\frac{1}{\alpha}, \quad (4)$$

in the limit of small α, whereas the amplitude of the potential is a constant equal to 2, allowing us to study the effect of a locally large first derivative. This is the potential introduced by Peyrard and Remoissenet (up to an irrelevant constant term) [22]. It is in contrast with the $\cos(2\pi x)$ choice for which the derivative is bounded by 2π. Its decomposition in the Fourier series is given by

$$V_\alpha(x) = 1 + 2\sinh\alpha\sum_{n=0}^{+\infty} e^{-\alpha n}[\cos(2\pi n x) - 1]. \quad (5)$$

The amplitudes of the successive harmonics decrease exponentially. It can also be viewed as a train of Lorentzians centered on the integers (see Appendix A).

We look for the equilibrium configurations $\{x_n\}$ that minimize the energy $W(\{x_n\})$. They must at least satisfy the equilibrium of forces equation,

$$\frac{\partial W}{\partial x_n} = 2x_n - x_{n-1} - x_{n+1} + \frac{K}{(2\pi)^2}V'_\alpha(x_n) = 0. \quad (6)$$

Note that if $\{x_n\}$ is a solution, $\{x_n + k\}$ where k is any integer is also a solution and $\{-x_n\}$ too, thanks to the parity of $V_\alpha(x)$, $V_\alpha(-x) = V_\alpha(x)$.

Aubry has rewritten the last equation by introducing the bond lengths $\ell_n \equiv x_{n+1} - x_n$,

$$\begin{aligned} x_{n+1} &= x_n + \ell_n, \\ \ell_{n+1} &= \ell_n + \frac{K}{(2\pi)^2}V'_\alpha(x_n + \ell_n). \end{aligned} \quad (7)$$

This defines a two-dimensional dynamical system where n is seen as a discrete time. It is known as the standard map when $V_\alpha(x)$ reduces to the cosine potential [1–3]. More generally, the nonlinear term of the map involves the derivative of the potential $V'_\alpha(x)$, not the potential itself, and may be large if

the derivative is large. Such maps have chaotic unbounded trajectories when K is large enough, but also periodic and quasiperiodic trajectories.

III. INCOMMENSURATE SOLUTIONS AND AUBRY TRANSITION

A. General background

In the absence of periodic potential, $K = 0$, the solution is simply given by

$$x_n = n\ell + \phi, \tag{8}$$

where the phase ϕ is arbitrary. This is the sliding phase of a trivial integrable model with continuous translation symmetry. This state satisfies the balance of forces and becomes the ground state when μ equals the lattice constant ℓ.

When $K \neq 0$, the problem is no longer simple but some exact properties of the ground states are known [2] (see also [23] and Appendix B). For a general class of models that includes the model we consider here (see Appendix B for the general conditions), Aubry and Le Daeron have shown that the ground state can be written

$$x_n = n\ell + \phi + u_n, \tag{9}$$

with a well-defined lattice constant,

$$\ell = \lim_{n\to\infty} \frac{x_n - x_0}{n}, \tag{10}$$

that can take any real value provided that μ is appropriately tuned. It is thus possible to work at fixed ℓ. Importantly, the distortions $\{u_n\}$ are bounded for the ground state and satisfy (see Appendix B)

$$|x_{n+1} - x_n - \ell| = |u_{n+1} - u_n| \leqslant 1. \tag{11}$$

In the ground state, the bond lengths are constrained not to be far from the average ℓ. ℓ, which is in units of the period of the potential, can be a rational or irrational number. In the first case,

$$\ell = \frac{r}{s}, \tag{12}$$

where r and s are two coprime integers, one has

$$x_{n+s} = x_n + r, \tag{13}$$

thus u_n is periodic with period s, $u_{n+s} = u_n$. In that case, the ground state is said to be commensurate and has a unit cell of size r admitting s atoms at positions x_n ($n = 1, \ldots, s$).

In the second case, when ℓ is an irrational number, the ground state is said to be incommensurate and can be viewed, physically, as a commensurate solution with a very large period s. The distortions can be written

$$u_n = g(n\ell + \phi), \tag{14}$$

where g is a periodic function with period 1 which is defined everywhere since $n\ell + \phi$ takes, modulo 1, all values in [0, 1]. The ground state then takes the special form

$$x_n = f(n\ell + \phi), \tag{15}$$

where $f(x) = x + g(x)$ is a strictly increasing function, called the envelope function. f depends on ℓ and on the various model parameters. The form (15) is exact for incommensurate ground states provided that the model fulfills the properties given in Appendix B. Importantly, f can be continuous or discontinuous: the change of regularity with model parameters is Aubry's breaking of analyticity (Aubry transition) [1,2].

For the model we consider, we define $K_c(\alpha)$ as the threshold of the Aubry transition: for $K < K_c(\alpha)$, the ground state is characterized by a *continuous* function f. This is the sliding phase. For $K > K_c(\alpha)$, f is *discontinuous*: this is the pinned phase. The threshold $K_c(\alpha)$ depends on the irrational ℓ. For the standard Frenkel-Kontorova model ($\alpha \to \infty$), it is empirically known that the maximal threshold occurs for $\ell = \frac{3-\sqrt{5}}{2} = 2 - \varphi \approx 0.3819660\ldots$ (where φ is the golden number) or, equivalently, at $\ell = \varphi - 1$, and $K_c(\infty) = 0.9716$ [24]. In the following, we examine the Aubry transition for $\ell = 2 - \varphi$.

At small K, the form of the solution (15) is coherent with the KAM theorem which applies to the dynamical system, Eq. (7). The KAM theorem ensures that, if ℓ is sufficiently irrational (there is a Diophantian condition [18]), the solution (8) of the integrable model ($K = 0$) remains a stable trajectory when the nonlinear potential is small enough, up to a change of variable f of the form (15). In this case, f is a *continuous* bijection. As a consequence, x_n mod 1 takes all values in [0, 1] just as in the $K = 0$ case: the KAM torus (here, the circle [0, 1]) with that irrational ℓ is preserved. It is known that the KAM theorem does not hold for arbitrary large K although (15) remains true with a discontinuous f. The threshold at which all the KAM tori cease to exist signals the transition to stochasticity [24] which is also the Aubry transition for $\ell = 2 - \varphi$.

B. Small K

We first mention that the continuous degeneracy of the ground states (8) at $K = 0$ is lifted at first order in perturbation theory for commensurate states but not for incommensurate states. We approximate the irrational number ℓ by a rational number $\ell = r/s$ (the larger the s, the better the approximation). At first order, the energy per atom of a unit cell noted $w^{(1)}$, assuming $\mu = \ell$, is given by

$$w^{(1)} = \frac{K}{s(2\pi)^2} \sum_{n=1}^{s} V_\alpha(n\ell + \phi) = \frac{K}{(2\pi)^2} \frac{\sinh \alpha}{\sinh \alpha s} V_{\alpha s}(s\phi) + C, \tag{16}$$

which goes to zero for all ϕ when $s \to +\infty$ (C is a constant independent of ϕ). It means that the energy barrier for translating the undistorted state by ϕ vanishes for an ideal incommensurate state at the lowest order (it is remarkable that it remains true at higher orders, as we will see below). Note that for a finite s, the energy depends on ϕ and the extrema are at $\phi = \frac{m}{2s}$ where m is an integer.

We now solve (6) by a perturbation theory at small K. In order to determine the distortions $u_n = g(n\ell + \phi)$ one can rewrite the extremal condition Eq. (6) as

$$g(x + \ell) + g(x - \ell) - 2g(x) = \frac{K}{(2\pi)^2} V'_\alpha(x + g(x)), \tag{17}$$

where $x = n\ell + \phi$, and use perturbation theory in K to determine the periodic function g. By using the Fourier series, one formally gets,

$$g(x) = \sum_{p=1}^{+\infty} \frac{A_p}{1 - \cos(2\pi p\ell)} \sin 2\pi px, \tag{18}$$

where A_p are some coefficients given, at first and second order in K, by

$$A_p^{(1)} = K \frac{\sinh \alpha}{2\pi} pe^{-\alpha p}, \tag{19}$$

$$A_p^{(2)} = K^2 \frac{\sinh^2 \alpha}{4\pi} \sum_{n \neq p} \frac{n^2(p-n)e^{-\alpha(|n|+|p-n|)}}{1 - \cos(2\pi(p-n)\ell)}, \tag{20}$$

where the last sum excludes all n such that $n - p = ks$ where k is an integer, if $\ell = r/s$.

Does the series Eq. (18) converge and what is the amplitude of the distortion?

For rational $\ell = r/s$, g has denominators $1 - \cos(2\pi p\ell) = 0$ when p is a multiple of s ($p = ks$), so that (18) is infinite, which means that Eq. (17) cannot be satisfied for all x (or all ϕ). The only possibility is to choose the special values $\phi = \frac{m}{2s}$, where m is any integer, which correspond to the extrema of $w^{(1)}$. In this case, when the denominator vanishes (for $p = ks$), the numerator vanishes too: $\sin(2\pi pn\ell + 2\pi p\phi) = \sin(2\pi kn + \pi km) = 0$. Consequently, (17) can be satisfied at these special points but not for all x or all ϕ, i.e., g is not defined everywhere, as expected for a commensurate solution.

For irrational ℓ, however, there are small denominators but they never vanish. For ℓ sufficiently irrational (this is where the Diophantian condition is important), it can be shown that the first-order series (18) converges, thanks to the exponential decrease of the harmonics [25]. The KAM theorem further ensures that higher-order series in K are convergent as well, provided that K remains small enough. In this case, g is a continuous function. The amplitude of the distortions δ defined as

$$\delta \equiv \mathrm{Max}_x\ |g(x)| \tag{21}$$

depends on K, α and ℓ. It is not simply proportional to K but depends on both α and ℓ in a complicated way because of the small denominators in (18). We now compute the distortions numerically, without relying on perturbation theory.

In Fig. 2, we plot two examples, for two different values of α at small K, of envelope functions g obtained numerically by a gradient descent algorithm that searches a zero of Eq. (6). When the algorithm converges (i.e., when the gradient is small), it gives a local minimum. In the regime of small K, there are no metastable states and starting from random configurations always produces the same state characterized by the envelope functions f and g as expected for the ground state. We thus obtain in this way, for a rational approximant of $2 - \varphi$ (typically $\ell = r/s = 377/987$), a periodic configuration $\{x_n\}$ ($n = 1, \ldots, s$) and distortions $\{u_n\}$ that we plot as a function of $n\ell$ mod 1 to define g. We then compare them with the perturbative results given by Eq. (18) up to the second order. Perturbation theory is in principle limited to $K \ll K_c(\alpha)$. By taking $K = 40\%K_c(\alpha)$, we observe in both cases of Fig. 2

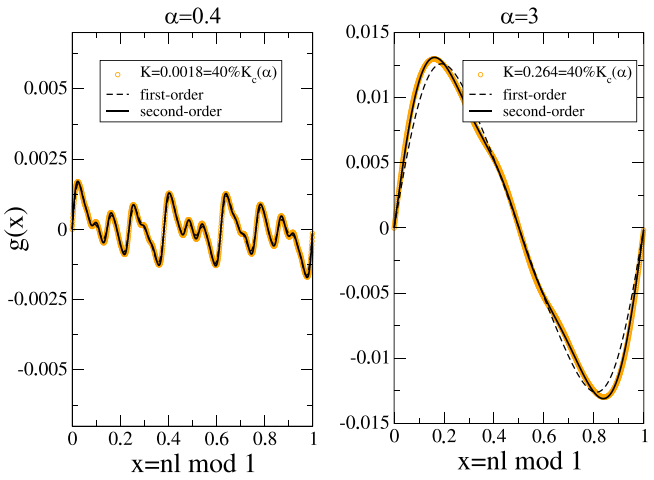

FIG. 2. Continuous envelope function g obtained by numerical [orange (light gray) points] and perturbative (black curves) [Eq. (18)] calculations at small $K = 40\%K_c(\alpha)$, for $\alpha = 0.4$ (left), and $\alpha = 3$ (right). Here, $\ell = 377/987 \approx 2 - \varphi$.

($\alpha = 0.4$ on the left and $\alpha = 3$ on the right) that perturbation theory is accurate, especially at second order. Small deviations are visible and disappear for smaller values of $K \ll K_c(\alpha)$, or, conversely, are amplified when $K \to K_c(\alpha)$. Note that the y scale is not the same, so the amplitude of the distortions δ is much smaller for small α (we have to take smaller values of K as well as remain at a fixed distance from the transition). The shape of the distortions also depends on α. When $\alpha \to +\infty$, we get the usual Frenkel-Kontorova model and only the first harmonic $p = 1$ is retained in (18). Thus, $g(x) = \gamma \sin 2\pi x$, $\gamma \equiv \frac{K}{4\pi} \frac{1}{1-\cos 2\pi\ell}$. This is already close to the result for $\alpha = 3$. On the other hand, for $\alpha \to 0$, more and more harmonics must be included, some of them with a large denominator but the numerical result remains small (thanks to smaller K). This is what is seen in Fig. 2 (left). The numerical result is thus in agreement with the KAM theorem and well approximated by the lowest order perturbation theory.

The distortions are small in this regime, particularly when α is small and K is appropriately reduced below the transition.

C. Large K

When K increases further, however, the previous perturbation theory fails. One can consider instead the anti-integrable limit $K \to \infty$ [26] and do perturbation theory in $1/K$. When $1/K = 0$, the solutions of Eq. (6) are given by

$$V'_\alpha(x_n) = 0, \tag{22}$$

so that x_n must be integers or half-integers. Since there is no determination of x_{n+1} from x_n, any series of integers (or half-integers or a mixing) $\{x_n\}$ is acceptable, i.e., can be random and very chaotic. Among the solutions, the following one,

$$x_n = [n\ell + \phi] + \tfrac{1}{2}, \tag{23}$$

where $[\ldots]$ is the integer part, is special. It is a ground state since all the atoms are at the bottoms of the potential (x_n mod $1 = 1/2$) and its average bond length is ℓ. It has the expected form given by Eq. (15) with a discontinuous envelope function given by $f(x) = [x] + 1/2$. Moreover, when

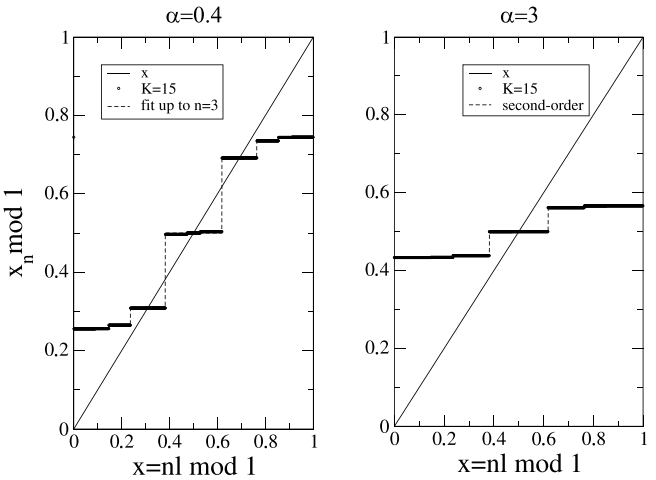

FIG. 3. Discontinuous envelope function f obtained by numerical and perturbative [Eq. (24)] calculations for large $K = 15, \alpha = 0.4$ (left), and $\alpha = 3$ (right). Here, $\ell = 377/987 \approx 2 - \varphi$. Note that it is impossible for these parameter values to distinguish the numerical result from the perturbative calculation.

$1/K$ is small but nonzero, a perturbative calculation in $1/K$ starting from Eq. (23) gives the ground state, whereas the other configurations give higher energy metastable states [26]. The ground state in perturbation in $1/K$ is thus obtained by

$$f(x) = [x] + \frac{1}{2} + \sum_{n=1}^{\infty} B_n([x + n\ell] + [x - n\ell] - 2[x]), \tag{24}$$

with coefficients B_n vanishing for large K. At first and second order in $1/K$, we find

$$B_n^{(1)} = \frac{1}{K}\left(\frac{1+\cosh\alpha}{\sinh\alpha}\right)^2 \delta_{n,1}, \tag{25}$$

$$B_n^{(2)} = \frac{1}{K^2}\left(\frac{1+\cosh\alpha}{\sinh\alpha}\right)^4 \delta_{n,2} - \frac{4}{K} B_n^{(1)}. \tag{26}$$

Thus $B_n = B_n^{(1)} + B_n^{(2)}$ (at second order) is a decreasing function of n. The perturbation theory is correct if the prefactor is small $\frac{1}{K}(\frac{1+\cosh\alpha}{\sinh\alpha})^2 \ll 1$, which needs, in the limit of small α, that $K\alpha^2/4 \gg 1$.

In Eq. (24), the periodic function $[x + a] + [x - a] - 2[x]$ is discontinuous at points na, for all n. Therefore, f is discontinuous at each point $x = \pm n\ell \bmod 1$, i.e., everywhere (since $n\ell \bmod 1$ is dense in $[0, 1]$ for ℓ irrational), with discontinuities that are functions of B_n.

In Fig. 3, the points are the atomic positions x_n mod 1 computed numerically for large K and plotted as a function of $n\ell$ mod 1. The gradient descent, started with a configuration sufficiently close to (24), converges to the ground state. We thus obtain the function ,f which is increasing and discontinuous, as expected for a ground state in this regime. For $\alpha = 3$ (Fig. 3, right), the second order result from Eq. (24) is shown as well (dashed line) and is a good approximation of the numerical result with main discontinuities at zero (obtained at zeroth order), $\pm\ell$ (first-order), and $\pm 2\ell$ mod 1 (second order). The other discontinuities obtained numerically are not reproduced at this order. The largest discontinuity at zero means

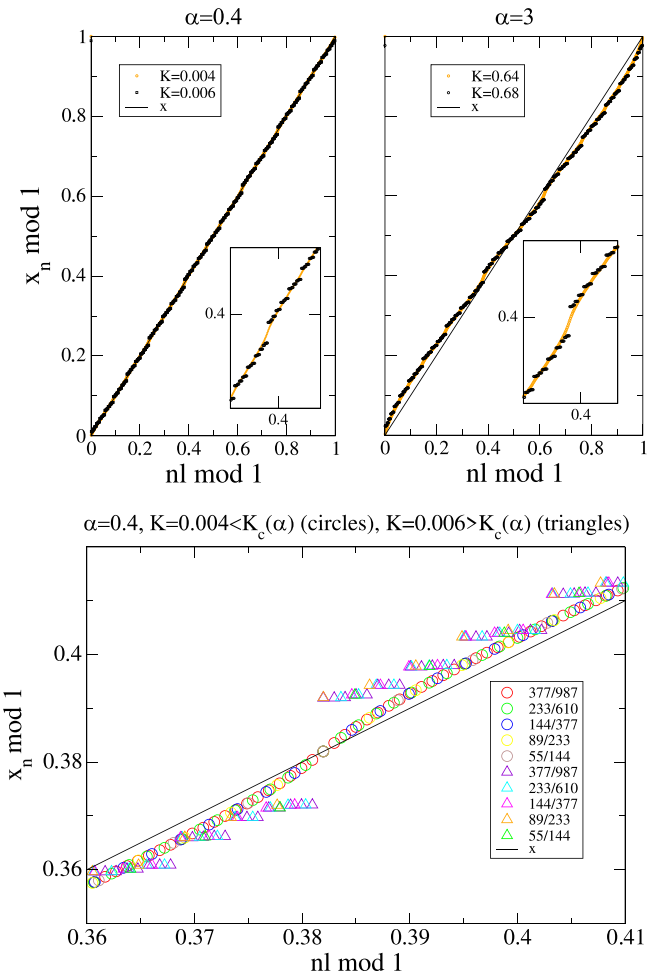

FIG. 4. Envelope functions f for $\alpha = 0.4$ (top left) and $\alpha = 3$ (top right) (zoom in the insets): the orange (light gray) points form a continuous curve for $K < K_c(\alpha)$, whereas the black points form a discontinuous one for $K > K_c(\alpha)$. Here, $\ell = r/s = 377/987 \approx 2 - \varphi$. Bottom: two examples of converged f just below (circles) and above (triangles) the Aubry transition for a series of fractions converging to $2 - \varphi$. The undistorted result $K = 0$ is given by $f(x) = x$.

that atoms avoid the maxima of the potential. For $\alpha = 0.4$ (Fig. 3, left), the lowest order perturbation theory already fails even for $K = 15$ because the prefactor is of order 1. The result shown by a dashed line is a fit that uses (24) and fitting parameters B_n up to $n = 3$, reproducing the main three discontinuities. The form of the solution (24) seems to remain accurate even though the parameters B_n are no longer given by perturbation theory. In both cases, we see that the distortions (departure from the $y = x$ line) are strong,

$$\delta \sim O(1). \tag{27}$$

The interpolation between the two previous regimes $K \to 0$ and $K \to \infty$ is through the Aubry transition.

D. Aubry transition

The simplest way to numerically show the existence of an Aubry transition is to follow the discontinuities of the envelope functions [12]. In Fig. 4, we show, as above,

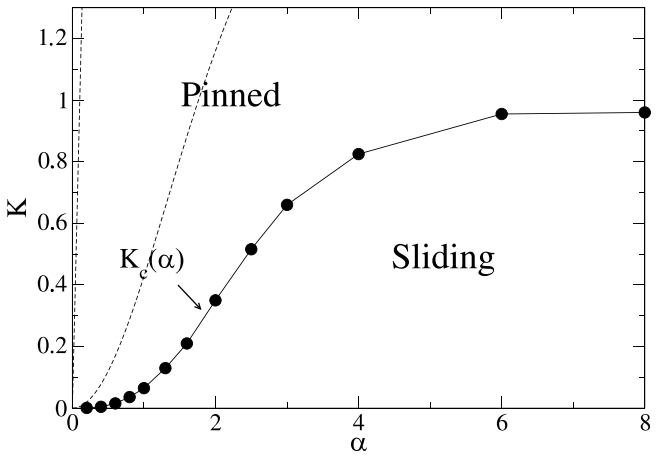

FIG. 5. Phase diagram with the sliding and pinned phase separated by the Aubry transition for incommensurate $\ell = 2 - \varphi$. The two dashed lines are crude analytical upper bounds of $K_c(\alpha)$ given by Eqs. (28) and (37).

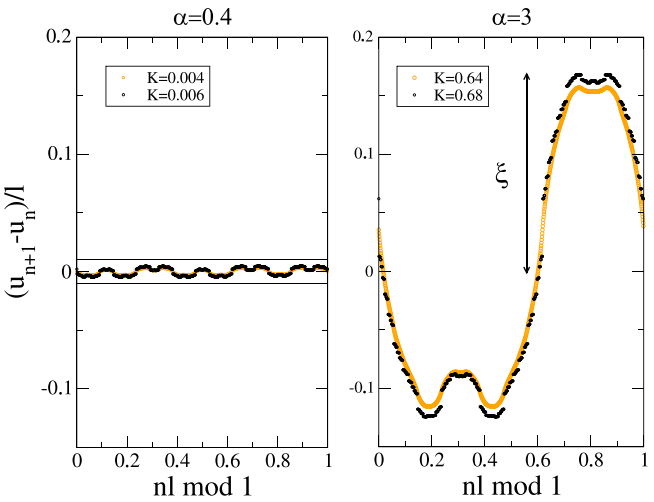

FIG. 6. Envelope functions h for the normalized bond lengths for $\alpha = 0.4$ (left) and $\alpha = 3$ (right): The orange (light gray) points form a continuous curve for $K < K_c(\alpha)$, whereas the black points form a discontinuous one for $K > K_c(\alpha)$. The amplitude is noted ξ. The horizontal bars on the left show $\pm$ 1%.

the numerically computed envelope function f. Since K is reduced compared with the results of Fig. 3, the distortions are reduced and $f(x)$ gets closer to $f(x) = x$. In each figure (top), two examples of values of K close to the threshold of the Aubry transition, $K_c(\alpha)$, are given. The orange (light gray) points ($K < K_c(\alpha)$) are the points of a continuous function (see insets for more clarity), just as in Fig. 2, and the black points ($K > K_c(\alpha)$) are that of a discontinuous function as in Fig. 3. We observe that the discontinuities close continuously so that the transition is a second order transition. Furthermore, we have checked the convergence of the envelope function for successive rational approximants of $2 - \varphi$. Two examples, one for $K < K_c(\alpha)$ and one for $K > K_c(\alpha)$, are given in Fig. 4 (bottom). Although, strictly speaking, there is no Aubry transition in commensurate systems, using such large values of s ensures a sharp change of continuity as a function of K. By locating the value of K for which the discontinuities close, we extract $K_c(\alpha)$ and the phase diagram showing the sliding phase $K < K_c(\alpha)$ and the pinned phase $K > K_c(\alpha)$ (Fig. 5). Note that $K_c(\alpha)$ vanishes when $\alpha \to 0$.

This can be simply understood by adapting an earlier argument [27] on the equilibrium of forces, Eq. (6). From the existence of a bound on the distortions expressed by Eq. (11), one obtains for the first part of Eq. (6) that $|2x_n - x_{n+1} - x_{n-1}| \leqslant 2$. In order to satisfy Eq. (6), its second part given by $\frac{K}{(2\pi)^2} V'_\alpha(x_n)$ cannot be arbitrary large. For irrational ℓ and sliding solution, x_n mod 1 takes all values in [0, 1] so that the maximum of $V'_\alpha(x)$, noted V'_m, is necessarily reached. Therefore, if $\frac{K}{(2\pi)^2} V'_m > 2$, some atoms in the sliding phase cannot be at equilibrium. In the limit of small α, given the expression of the maximum of the derivative (4), we get that, for

$$K > \frac{8\pi^2}{V'_m} = \frac{16\pi\sqrt{3}}{9}\alpha \qquad (\alpha \to 0), \tag{28}$$

it is impossible to maintain the balance of forces in the sliding phase. In particular, when $\alpha = 0$ the right-hand side vanishes so that

$$K_c(0) = 0. \tag{29}$$

At the limit $\alpha = 0$ the potential is discontinuous at $x = 0$ and the KAM torus is destroyed at that point. This qualitative argument confirms that in the limit of small α, the pinned phase should be favored at small K. Importantly, one sees that if the derivative of the potential V'_m is *somewhere* strong enough, the sliding phase no longer exists because the atoms that experience that strong force (some necessarily do in the sliding phase) cannot be at equilibrium: the Aubry transition threshold of the pinned state is reduced. The bound in (28) is in fact a very crude estimate of $K_c(\alpha)$ (see the steep dashed line in Fig. 5). A better bound represented by the dashed curve in Fig. 5 will be given in Sec. IV.

In order to get some quantitative insights into how large the distortions can be near and at the Aubry transition when the phase is pinned, we also compute numerically the bond lengths,

$$\ell_n = \ell + (u_{n+1} - u_n). \tag{30}$$

Recall that the average bond length is $\frac{1}{s}\sum_{n=1}^{s} \ell_n = \ell$ so that $(u_{n+1} - u_n)/\ell$ measures the amplitude of the distortion with respect to the average. We define another envelope function h by $(u_{n+1} - u_n)/\ell = h(n\ell + \phi)$. Its amplitude

$$\xi \equiv \mathrm{Max}_x\, |h(x)| \tag{31}$$

gives an idea of how much distorted the structure is. In Fig. 6, we show $(u_{n+1} - u_n)/\ell$ as a function of $n\ell$ mod1 (i.e., h) for two values of K, one for $K < K_c(\alpha)$ (continuous curves), the other for $K > K_c(\alpha)$ (discontinuous curve). For large values of α ($\alpha = 3$ in Fig. 6, right), the amplitude is large. On the contrary, for small α ($\alpha = 0.4$ in Fig. 6, left), we observe that the distortions are well within 1 % of the bond length (the two horizontal lines correspond to ± 1 %). The amplitude ξ is reported in Fig. 7 as a function of α at $K = K_c(\alpha)$. For large α, the maximal distortion at the transition is 23% (Frenkel-Kontorova limit). For smaller values of α, ξ can be arbitrary small. It can also be seen qualitatively in Fig. 4 that for small

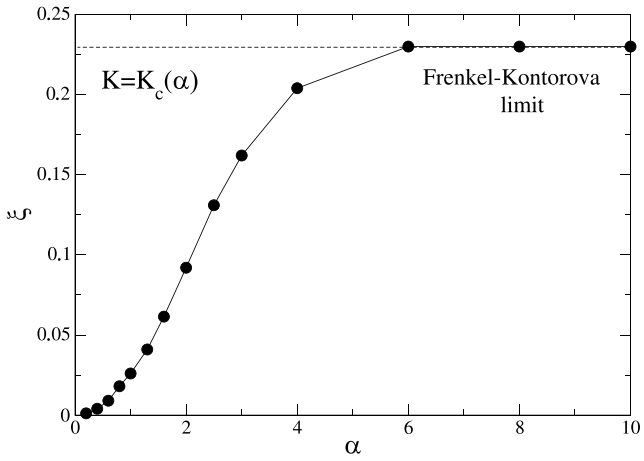

FIG. 7. Maximal distortion ξ (see definition in Fig. 6) as a function of the potential shape parameter α, at the Aubry transition. At small α, ξ can be arbitrarily small and reaches 23% (dashed line) at large α (Frenkel-Kontorova limit).

α (left), the distortions are very small and f is very close to the undistorted result $f(x) = x$, whatever the values of K across and near the Aubry transition.

The important conclusion is that it is not necessary to have large distortions to have an Aubry transition or be in the pinned phase. In particular, if $\alpha = 0$, so that the potential is discontinuous, $K_c(0) = 0$ as we have shown above: the system is immediately in the pinned phase. Yet the potential is flat almost everywhere so that there is no distortion. This extreme situation remains somehow valid at small α, as shown here. It is replaced by a pinned phase with small distortions.

IV. STABILITY AND PHONON SPECTRUM

We now examine the stability of the solution and the phonon spectrum, in particular its gap that vanishes at the Aubry transition, defining the zero-energy phason mode of the continuous ground state manifold for $K < K_c(\alpha)$. For this, we add the kinetic energy of the atoms

$$H = \frac{1}{2}\sum_n \dot{x}_n^2 + W(\{x_n\}), \tag{32}$$

and write

$$x_n = x_n^{eq} + \epsilon_n, \tag{33}$$

where $x_n^{eq} = n\ell + u_n$ is the equilibrium position in the ground state previously obtained and ϵ_n a sufficiently small deviation to expand the energy:

$$W(\{x_i\}) = W\left(\{x_i^{eq}\}\right) + \frac{1}{2}\sum_{n,m}\frac{\partial^2 W}{\partial x_n \partial x_m}\epsilon_n\epsilon_m. \tag{34}$$

The nonzero partial derivatives are given by

$$\frac{\partial^2 W}{\partial x_n^2} = 2 + \frac{K}{(2\pi)^2}V_\alpha''\left(x_n^{eq}\right), \tag{35}$$

$$\frac{\partial^2 W}{\partial x_n \partial x_{n\pm1}} = -1, \tag{36}$$

where $V_\alpha''(x)$ is given in Appendix A. Note that for the equilibrium phase to be a minimum of the energy, the matrix on the right-hand side of (34) must be definite positive. The (Sylvester) criterion implies in particular that all diagonal elements must be positive [27]. In the sliding phase, all values of $V_\alpha''(x_n)$ are attained, in particular its minimum $V_\alpha''(0) < 0$. When K increases, $2 + \frac{K}{(2\pi)^2}V_\alpha''(0)$ becomes negative and the matrix is no longer definite positive (the sliding phase is unstable), i.e., when

$$K > \frac{2(2\pi)^2}{|V_\alpha''(0)|} = 2\frac{\cosh\alpha - 1}{\cosh\alpha + 1}. \tag{37}$$

This analytical bound is a crude approximation but is in agreement with the numerical result giving $K_c(\alpha)$ (see the dashed curve in Fig. 5 for a comparison). It could be refined by using higher-order minors [27] but it is not necessary here. We find again that when $\alpha \ll 1$, the sliding phase must be unstable above $K \sim \alpha^2/2$ which is small.

To compute the phonons we now assume a commensurate state with $\ell = r/s$ and that $\epsilon_n = \bar{\epsilon}_n e^{i(kn-\omega_k t)}$ (the amplitude $\bar{\epsilon}_n$ is periodic with a period s) and obtain an $s \times s$ matrix:

$$M_{n,m} = -\omega_k^2\delta_{n,m} + \frac{\partial^2 W}{\partial x_n \partial x_m}. \tag{38}$$

The matrix M has also the nonzero end points $\frac{\partial^2 W}{\partial x_s \partial x_1} = -e^{\pm iks}$ for $\ell \neq 0, 1/2$. The diagonalization of M gives the phonon energies $\omega(k)$. For the integrable point $K = 0$, the spectrum is simply given by the standard expression:

$$\omega(k) = 2\left|\sin\frac{k}{2}\right|. \tag{39}$$

In the opposite anti-integrable limit $K \to +\infty$, the atoms are all at the bottoms of the potential, $V_\alpha''(x_n) = V_\alpha''(1/2)$ and the dispersion relation is

$$\omega(k) = \sqrt{\Delta^2 + 4\sin^2\frac{k}{2}}, \tag{40}$$

with gap Δ given by $\Delta^2 = \frac{K}{(2\pi)^2}V_\alpha''(1/2) = K\frac{\sinh^2\alpha}{(1+\cosh\alpha)^2}$ [see (A9)]. Note that the anti-integrable limit applies precisely when $\Delta \gg 1$ (see Sec. III C). In this case, the spectrum consists of a single (gapped) band.

In between, for $K \neq 0$, the spectrum $\omega(k)$ is computed numerically. Two examples are given in Fig. 8 for $\ell = 377/987 \approx 2 - \varphi$ and two different values of α. $\omega(k)$ is represented in the half-extended Brillouin zone, i.e., for k in $[0, \pi]$.

In both cases, the spectra of the sliding phases [$K < K_c(\alpha)$, orange (light gray) curves] have no zero-energy gap. This is the consequence of the existence of a continuous manifold of ground states. The associated zero-energy mode is the phason, which becomes gapped in the pinned phase above the Aubry transition $K > K_c(\alpha)$ (black curves). Note that the parameters K in gapped cases are chosen so that the gap is the same in both figures (see the black curves in the insets). The values of K (0.008 and 0.71) differ by almost two orders of magnitude. Measuring experimentally a certain gap is therefore not sufficient to tell what the amplitude K of the potential is.

For small α (top), the distortions and the values of K at the Aubry transition are small, so that the spectrum is closer to the

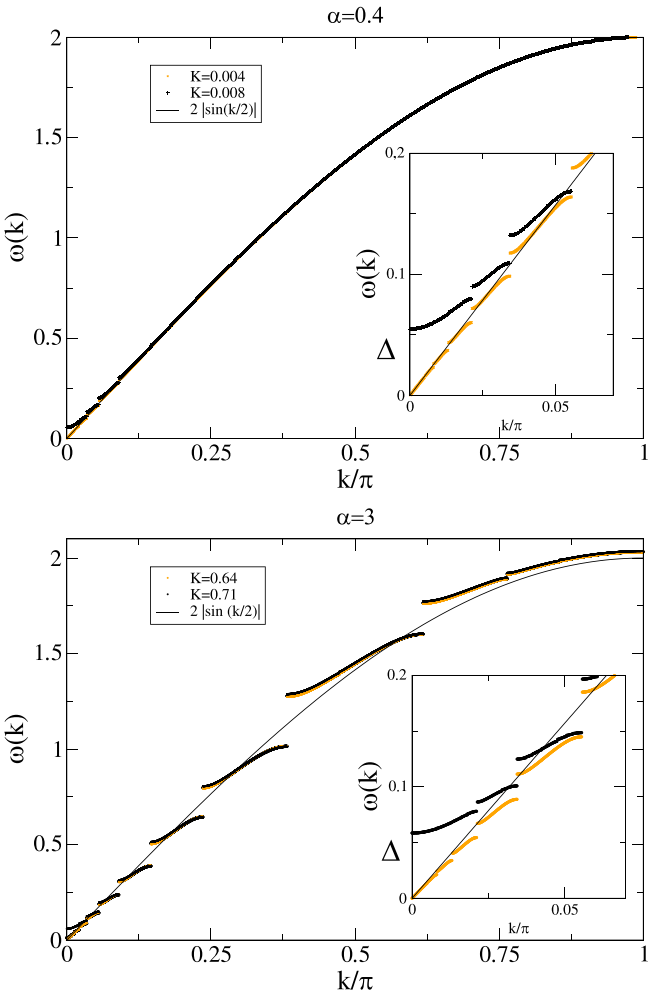

FIG. 8. Phonon spectrum for $\alpha = 0.4$ and $\alpha = 3$ (zoom in the insets). For $K < K_c(\alpha)$ [orange (light gray) curves], the spectrum has no gap at $k = 0$ (phason mode). For $K > K_c(\alpha)$, the spectrum has a gap at $k = 0$ (black curves). Here $\ell = 377/987$.

standard phonon spectrum (39). For large α (bottom), there are much larger gaps at higher energies. Since the periodic potential mixes modes with k and $k \pm 2\pi p\ell$ (where p is an integer), one expects gaps at every level crossing. One sees that for small α the high-energy gaps are all very small while they are large when α is large. This simply reflects the strength of the distortions. It makes a qualitative difference which may help to distinguish experimentally between strongly nonlinear potentials (small α) and harmonic potentials (large α).

V. CONCLUSION

The distortions of incommensurately modulated phases are not necessarily as strong as what the Frenkel-Kontorova model or charge-density wave models suggest when pinning occurs. When the smoothness conditions of the nonlinear perturbation are progressively suppressed, i.e., here when the derivative of the potential (the mechanical force) becomes locally strong enough, the pinning threshold $K_c(\alpha)$ is reduced. This is coherent with the fact that the KAM theorem no longer applies to potentials with some singularities. At the same time, the distortions can be weak if the potential is flatter in large portions of space. This is what we have provided evidence for by considering a simple modified potential in which these two regions coexist, a situation that does not occur in the standard Frenkel-Kontorova model where the derivative of the potential is bounded. The two effects, pinning and distortions, are therefore not necessarily related. This opens a wide range of applicability of the Aubry transition since distortions need not be large in incommensurate pinned phases.

We therefore emphasize that observing experimentally small incommensurate distortions ξ (as in charge-density waves) does not generally imply that the phase should be sliding. This is only true for the standard Frenkel-Kontorova model. It does not imply that perturbation theory, which leads to the sliding phase, is applicable because it is highly resonant due to the small denominators. The small parameter of the perturbation theory is $K/K_c(\alpha)$, not ξ. For the standard Frenkel-Kontorova model, we have simultaneously $\xi \ll 1$ and $K/K_c \ll 1$. However, in general cases, ξ may be small while $K/K_c(\alpha)$ remains large, so that the perturbation theory does not apply.

ACKNOWLEDGMENT

We would like to thank G. Masbaum of the Institut de Mathématiques de Jussieu (Paris) for stimulating discussions on various mathematical problems concerning our physical models.

APPENDIX A: MODIFIED POTENTIAL

The modified potential considered here depends on a real parameter α and is written in three different forms:

$$V_\alpha(x) = \frac{\cosh\alpha\cos(2\pi x) - 1}{\cosh\alpha - \cos(2\pi x)} \tag{A1}$$

$$= 1 + 2\sinh\alpha \sum_{n=0}^{+\infty} e^{-\alpha n}[\cos(2\pi n x) - 1] \tag{A2}$$

$$= \sum_{n=-\infty}^{+\infty} \frac{2\alpha\sinh\alpha}{[2\pi(x-n)]^2 + \alpha^2} - \cosh\alpha. \tag{A3}$$

It is easy to prove these equalities. For example, starting from (A3) and using Poisson's formula for $h(x) \equiv \frac{\alpha}{4\pi^2x^2+\alpha^2}$,

$$\sum_{n=-\infty}^{+\infty} h(x-n) = \sum_{p=-\infty}^{\infty} \hat{c}_p e^{2ip\pi x} \tag{A4}$$

with

$$\hat{c}_p = \int_{-\infty}^{+\infty} h(x) e^{-2i\pi px} dx = \frac{1}{2} e^{-|p|\alpha}, \tag{A5}$$

we find (A2). Then, by resummation of the Fourier series (A2), we get (A1).

The first and second derivatives of the potential are given by

$$V'_\alpha(x) = -2\pi \frac{\sinh^2\alpha\sin(2\pi x)}{[\cosh\alpha - \cos(2\pi x)]^2}, \tag{A6}$$

$$V''_\alpha(x)/(2\pi)^2 = \sinh^2\alpha \frac{1+\sin^2(2\pi x)-\cosh\alpha\cos(2\pi x)}{[\cosh\alpha-\cos(2\pi x)]^3}. \tag{A7}$$

The first derivative has a maximum which, for small α, lies at $x_0 = \alpha/(2\pi\sqrt{3})$, so that $V'_\alpha(x_0) = \frac{9\pi}{2\sqrt{3}}\frac{1}{\alpha}$ which is large when α is small. We also have

$$V''_\alpha(0)/(2\pi)^2 = -\frac{\cosh\alpha+1}{\cosh\alpha-1} \tag{A8}$$

$$V''_\alpha(1/2)/(2\pi)^2 = \frac{\sinh^2\alpha}{(1+\cosh\alpha)^2}. \tag{A9}$$

APPENDIX B: SOME EXACT RESULTS

The energy given by Eq. (1) can be written as:

$$W(\{x_n\}) = \sum_n H(x_{n+1}, x_n) - \mu\sum_n (x_{n+1}-x_n), \tag{B1}$$

with the twice differentiable function H:

$$H(x,y) = \tfrac{1}{2}[(x-y)^2 + V_\alpha(x) + V_\alpha(y) + \mu^2]. \tag{B2}$$

Because the function H satisfies a convexity condition,

$$\frac{\partial H}{\partial x \partial y} = -1 < 0, \tag{B3}$$

together with a condition of periodicity,

$$H(x+1, y+1) = H(x,y), \tag{B4}$$

the model (1) belongs to the class of Frenkel-Kontorova models studied in [2]. Slightly more general conditions are given in Ref. [23]. For such models, some exact results are known, in particular:

(1) A ground state with a given ℓ exists (for some μ) and is characterized, in the incommensurate case, by a strictly increasing envelope function (15).

(2) It is always possible to choose ϕ such that the ground state solution x_n and $n\ell+\phi$ belong to the same well of the periodic potential.

(3) An incommensurate ground state with a given ℓ can be obtained as a limit of a sequence of commensurate ground states with average bond lengths $\ell_i \to \ell$.

(4) In any ground state with a given ℓ, the distortions are bounded and satisfy Eq. (11) [28].

[1] S. Aubry, *Solitons and Condensed Matter Physics*, edited by A. R. Bishop, T. Schneider, Springer Series in Solid-State Sciences Vol 8. (Springer, Berlin, Heidelberg, 1978).

[2] S. Aubry and P. Y. Le Daeron, Physica D **8**, 381 (1983).

[3] J. N. Mather, Topology **21**, 457 (1982).

[4] O. M. Braun and Y. S. Kivshar, *The Frenkel-Kontorova Model, Concepts, Methods, and Applications* (Springer-Verlag, 2004).

[5] T. Dauxois and M. Peyrard, *Physics of Solitons* (Cambridge University Press, Cambridge, 2004).

[6] M. Dienwiebel, G. S. Verhoeven, N. Pradeep, J. W. M. Frenken, J. A. Heimberg, and H. W. Zandbergen, Phys. Rev. Lett. **92**, 126101 (2004).

[7] F. Lançon, J. Ye, D. Caliste, T. Radetic, A. M. Minor, and U. Dahmen, Nano Lett. **10**, 695 (2010).

[8] A. Socoliuc, R. Bennewitz, E. Gnecco, and E. Meyer, Phys. Rev. Lett. **92**, 134301 (2004).

[9] A. Bylinskii, Nat. Mater. **15**, 717 (2016).

[10] T. Brazda, A. Silva, N. Manini, A. Vanossi, R. Guerra, E. Tosatti, and C. Bechinger, Phys. Rev. X **8**, 011050 (2018).

[11] P. Y. Le Daeron and S. Aubry, J. Phys. C: Solid State Phys. **16**, 4827 (1983).

[12] S. Aubry and P. Quémerais, in *Low Dimensional Electronic Properties of Molybdenum bronzes and Oxides*, edited by C. Schlenker (Kluwer Academic Publishers, Dordrecht, 1989), p. 295.

[13] *Electronic Properties of Inorganic Quasi-one Dimensional Compounds*, edited by P. Monceau (Reidel Publishing Company, Dordrecht 1985).

[14] J.-P. Pouget and E. Canadell, Rep. Prog. Phys. **87**, 026501 (2024).

[15] O. Cépas and P. Quémerais, SciPost Phys. **14**, 051 (2023).

[16] See, for example, H. Scott Dumas, *The KAM Story, a Friendly Introduction to the Content, History and Significance of Classical Kolmogorov-Arnold-Moser Theory* (World Scientific, New Jersey, 2014).

[17] S. A. Brazovskii, I. E. Dzyaloshinskii, and I. M. Krichever, Soviet Phys. JETP **56**, **1**, 212 (1982).

[18] Other conditions apply, in particular the perturbation must also be 'smooth enough'. If it has some singularities (possibly in higher order derivatives), KAM theorem does not apply. To know what the optimal smoothness conditions are, see Ref. [16].

[19] A. Milchev, Phys. Rev. B **33**, 2062 (1986).

[20] C.-I. Chou, C. L. Ho, B. Hu, and H. Lee, Phys. Rev. E **57**, 2747 (1998).

[21] W. Quapp and J. M. Bofill, Eur. Phys. J. B **93**, 227 (2020).

[22] M. Peyrard and M. Remoissenet, Phys. Rev. B **26**, 2886 (1982).

[23] V. Bangert, in *Dynamics Reported*, edited by U. Kirchgraber and H. O. Walther (John Wiley & Sons, Chichester, 1988), Vol. 1.

[24] J. Greene, J. Math. Phys. **20**, 1183 (1979).

[25] The proof of the convergence of such series with small denominators and Diophantian conditions is part of KAM theorem, see, for example, Ref. [16] or C. E. Wayne, in *Dynamical Systems and Probabilistic Methods in Partial Differential Equations*, edited by P. Deift, C. D. Levermore and C. E. Wayne, Lectures in Applied Mathematics Vol. 31 (American Mathematical Society, Providence/Rhode Island, 1996).

[26] S. Aubry and G. Abramovici, Physica D **43**, 199 (1990).

[27] S. Aubry, Physica D **7**, 240 (1983).

[28] This is proved in Appendix D of Ref. [2] for commensurate ground states (and at the limit for incommensurate ground states), formula D.2 applied for $m = n+1$.